74Bur: B.P. Burylev, N.N. Fedorova, and L.Sh. Tsemekhman, "Phase Diagrams of Cu-S, Cu-Se and Cu-Te Systems", *Zh. Neorg. Khim., 19*, 2283-2285 (1974) in Russian; TR: *Russ. J. Inorg. Chem., 19*(8), 1249-1250 (1974). (Equi Diagram; Experimental)

74Dum: A. Dumon, A. Lichanot, and S. Gromb, "Study of Cu-S Phase Diagram in Compositional Area $Cu_{2.000}S$-$Cu_{1.960}S$", *J. Chim. Phys., 71*(3), 407-414 (1974) in French. (Equi Diagram; Experimental; #)

74Mil: K.C. Mills, *Thermodynamic Data for Inorganic Sulphides, Selenides and Tellurides*, Butterworths, London (1974). (Thermo; Compilation)

***74Rau:** H. Rau, "Homogeneity Range of Cubic High Temperature Cuprous Sulfide (Digenite)", *J. Phys. Chem. Solids, 35*, 1415-1424 (1974). (Equi Diagram, Thermo; Experimental; #)

75Gor: S.S. Gorelik, A.N. Dubrovina, R.Kh. Leksina, T. Turdaliev, and Yu.M. Ukrainskii, "Dilatometric and X-Ray Investigation of Copper Chalcogenides at 20-700 °C", *Izv. Akad. Nauk SSSR, Neorg. Mater., 11*(1), 28-32 (1975) in Russian; TR: *Inorg. Mater., 11*(1), 21-24 (1975). (Crys Structure; Experimental)

76Bal: C.W. Bale and J.M. Toguri, "Thermodynamics of Cu-S, Fe-S and Cu-Fe-S Systems", *Can. Met. Quart., 15*(4), 305-318 (1976). (Equi Diagram, Thermo; Experimental)

76Eva: H.T. Evans, Jr. and J.A. Konnert, "Crystal Structure Refinement of Covellite", *Am. Miner., 61*, 996-1000 (1976). (Crys Structure; Experimental)

***76Kel:** H.H. Kellog, "Thermochemical Modelling of Molten Sulfides", *Physical Chemistry in Metallurgy*, R.M. Fischer, R.A. Oriani, and E.T. Turkdogan, Ed., U.S. Steel Res. Lab., Monroeville, PA, 49 (1976). (Thermo; Experimental)

76Nag: M. Nagamori, "A Thermodynamic Study of Digenite Solid Solution ($Cu_{2-\delta}S$) at 600 to 1000 °C and a Statistical Thermodynamic Critique on General Nonstoichiometry", *Met. Trans., 7B*, 67-80 (1976). (Thermo; Experimental)

76Pot: R.W. Potter, II and H.T. Evans, Jr., "Definitive X-ray Powder Data for Covellite, Anilite, Djurleite and Chalcocite", *U.S. Geol. Survey J. Res., 4*, 205-212 (1976). (Crys Structure; Experimental)

76Vai: J.C. Vaissiere and F.M. Roche, "Contribution to Study of Phase Diagram of Cu_xS ($1.75 \leq x \leq 2$) Between 10 and 200 °C", *Mater. Res. Bull., 11*(7), 851-856 (1976). (Equi Diagram; Experimental)

***77Pot:** R.W. Potter, II, "An Electrochemical Investigation of the System Cu-S", *Econ. Geol., 72*(8), 1524-1542 (1977). (Equi Diagram, Meta Phases, Thermo; Experimental; #)

79Jud: V.P. Judin and E. Eerola, "Thermodynamics of Metallic Impurities in Cu-Saturated Cu-Sulfide Melts", *Scand. J. Metall., 8*, 128-132 (1979). (Thermo, Equi Diagram; Experimental; #)

79Kub: O. Kubaschewski and E.L. Evans, *Metallurgical Thermochemistry*, 5th ed., Pergamon Press, NY (1979). (Thermo; Compilation)

79Lar: J.M. Larrain, L.L. Sang, and H.H. Kellog, "Thermodynamic Properties of Cu-S Melts", *Can. Met. Quart., 18*, 395-400 (1979). (Thermo, Equi Diagram; Theory)

79Mou: M. Moulki and J. Osterwald, "Miscibility Gap between Liquid Cu and Liquid Cu-Sulfide", *Z. Metallkd., 70*(12), 808-810 (1979) in German. (Equi Diagram; Experimental)

79Sha: R.C. Sharma and Y.A. Chang, "A Thermodynamic Equation of State for Digenite, $Cu_{2-\delta}S$", *Chin. J. Mater. Sci., 11*(1), 58-62 (1979). (Thermo; Theory)

***80Sha:** R.C. Sharma and Y.A. Chang, "A Thermodynamic Analysis of Cu-S System", *Met Trans., 11B*, 575-583 (1980). (Thermo, Equi Diagram; Theory; #)

81BAP: *Bull. Alloy Phase Diagrams, 2*(1), 145-146 (1981), quoting melting points of elements on the 1968 temperature scale. (Equi Diagram; Compilation; #)

81Hub: C.R. Hubbard and D.L. Calvert, "The Pearson Symbol", *Bull. Alloy Phase Diagrams, 2*(2), 153-157 (1981). (Crys Structure; Review)

*Indicates key paper.
#Information from this paper used in drawing evaluated phase diagrams.

Cu-S evaluation contributed by **D.J. Chakrabarti** and **D.E. Laughlin**, Department of Metallurgical Engineering and Materials Science, Carnegie-Mellon University, Pittsburgh, PA 15213, USA. Work was supported by the International Copper Research Association, Inc., (INCRA) and the Department of Energy through the Joint Program on Critical Compilation of Physical and Chemical Data coordinated through the Office of Standard Reference Data (OSRD), National Bureau of Standards. Literature searched through 1980. Professor Laughlin is the ASM/NBS Data Program Category Editor for binary copper alloys.

The Al-In (Aluminum-Indium) System

26.98154 114.82

By J.L. Murray
National Bureau of Standards

Equilibrium Diagram

The Al-In system is characterized by liquid-phase immiscibility below a critical point, a monotectic reaction of (Al) with the two liquids, and a eutectic reaction in which the last In-rich liquid solidifies. There are conflicting data on the miscibility gap near the critical point. By means of thermodynamic analysis and consideration of nonclassical critical phenomena, we suggest possible sources of error in interpreting experiments.

The assessed phase diagram, shown in Fig. 1 and 2, is based on thermodynamic optimization calculations using enthalpy of mixing and phase boundary data. This calculation provides an upper bound on the critical temperature because it uses a classical model for the Gibbs energies and predicts classical critical exponents that are known to be incorrect. The calculated miscibility gap has been adjusted near the critical point to give a more nearly correct exponent for the phase boundaries. In Fig. 3, the calculation is compared to the assessed miscibility gap and to experimental data, including data omitted in the optimizations.

The solid phases of the system are: (1) the fcc (Al) solid solution, which dissolves about 0.045 at.% In, and (2) the (In) solid solution, which dissolves very little Al. The invariant points defining the topology of the diagram are listed in Table 1.

Monotectic Equilibrium and Al-Rich Liquidus. The monotectic point is 4.7 ± 0.3 at.% In and 639 ± 1 °C. The monotectic composition is taken from [81Gru], who analyzed a

Fig. 1 Al-In Assessed Diagram

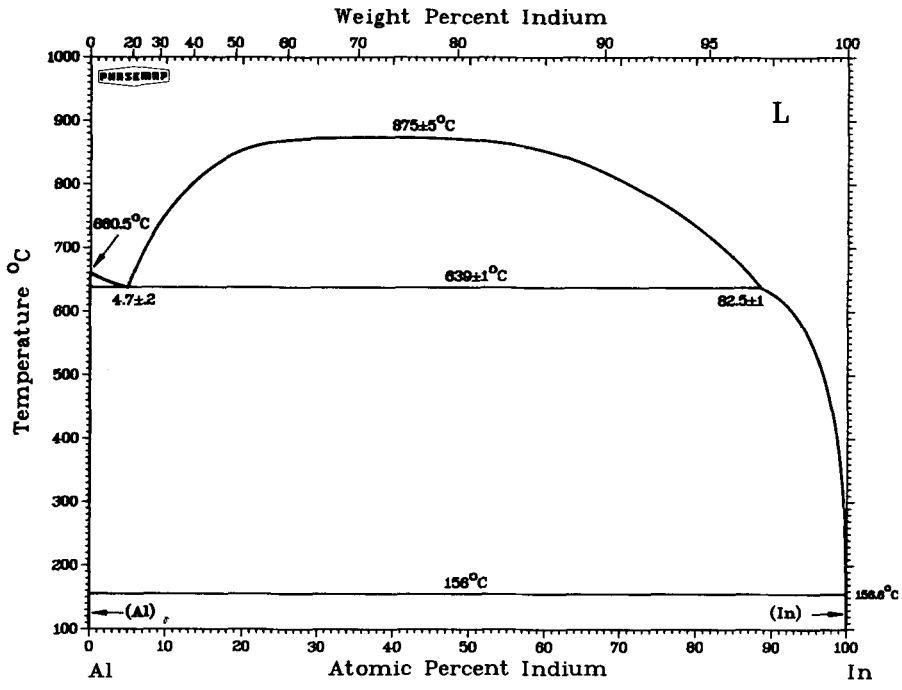

J.L. Murray, 1983.

Fig. 2 Enlargement of the (Al) Liquidus and Monotectic Point with Experimental Data

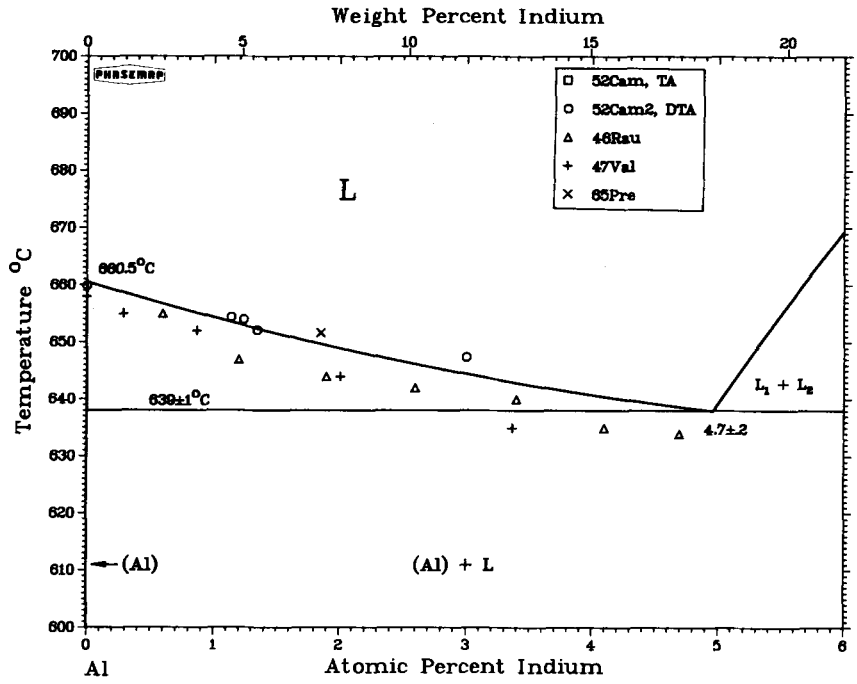

J.L. Murray, 1983.

series of alloys exhibiting a monotectic microstructure. This value is consistent with thermal analysis measurements of the Al-rich liquidus.

[49Por, 47Val, 46Rau, 52Cam] made thermal analysis and/or DTA measurements of the (Al) liquidus. The data are compared to the assessed diagram in Fig. 2. All measurements agree within ±7 °C. [47Val] found the melting point of pure Al to be 658 °C, indicating that impurities were the cause of the relatively low melting points in this work. Thermal analysis data of [52Cam] lie about 7 °C higher than their DTA data and are inconsistent with

Fig. 3 Comparison of the Calculated and Modified (Assessed) Critical Regions

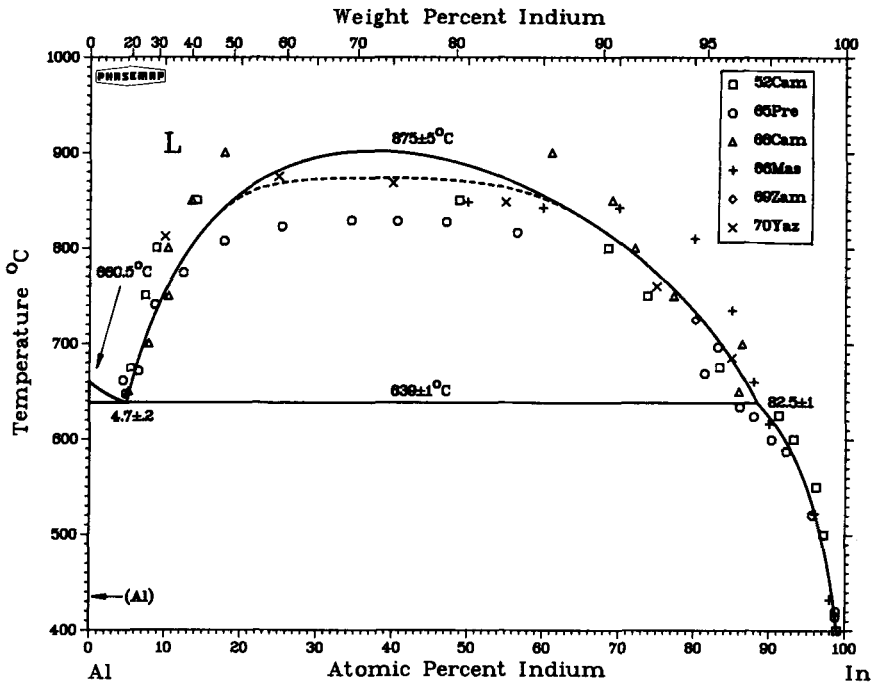

J.L. Murray, 1983.

Table 1 Three-Phase Equilibria and Congruent Transformations

Phases	Compositions, at.% In			Temperature, °C	Reaction type
$L_1 \rightleftarrows (Al) + L_2$	4.7 ± 0.3	0.045 ± 0.005	88.5 ± 1	639 ± 1	Monotectic
$L_2 \rightleftarrows (Al) + (In)$	~100	~0	~100	156	Eutectic
$L \rightleftarrows L_1 + L_2$		~38 ± 5		875 ± 5	Critical
$L \rightleftarrows (Al)$		0		660.452	Pure component
$L \rightleftarrows (In)$		100		156.634	Pure component

van't Hoff's law. Of [46Rau] and [52Cam], the data of [52Cam] lie higher in temperature and are expected to be more correct because of the possibility of undercooling by [46Rau]. Monotectic arrests were observed in the range 634 to 640 °C ([46Rau], 634 °C; [47Val], 635 °C; [48Kle], 640 °C; [52Cam], 638.6 °C). Again, higher values are preferred.

In our thermodynamic calculations, we found that we could easily reproduce a monotectic temperature between 635 and 639 °C, but that the monotectic composition was a more sensitive test of the accuracy of the Gibbs energies. The monotectic composition was, therefore, heavily weighted among the experimental data. The calculated monotectic point lies at 4.96 at.% In and 638 °C. The liquidus lies between the data of [52Cam] and [46Rau], within 6 °C of the [46Rau] data and 3 °C of the [52Cam] data. The calculated Al-rich liquidus is compared to the experimental data in Fig. 2.

Liquid Immiscibility. Experimental determinations of the miscibility gap disagree with one another by as much as 115 °C near the critical temperature. Measurements are grouped in three sets: (1) direct sampling of two liquid layers within the two-phase region [52Cam, 66Cam]; (2) DTA [65Pre]; and (3) emf and enthalpy of mixing measurements [69Yaz, 70Yaz, 66Mas, 77Gir, 63Wit]. Miscibility gap data are summarized in Table 2. [66Cam] reported the highest critical temperature, 945 °C; [52Cam, 70Yaz, 66Mas] reported intermediate values, and [69Pre] reported the lowest value, 830 °C. We tentatively place the critical temperature at 875 ± 5 °C, based on an analysis of the most probable experimental pitfalls for these techniques and thermodynamic calculations.

The direct sampling experiments of [52Cam, 66Cam] disagree with one another. [52Cam] sampled and analyzed the two liquid layers up to 850 °C. They performed a quenching experiment from 900 °C and found that no separation into two liquid layers had occurred during the homogenization treatment. Although phase separation during quenching may cause a single-phase alloy to appear to be two-phase, the reverse is unlikely. We conclude from the quenching experiment that the critical temperature is below 900 °C. [66Cam] used a different, apparently slower, technique for extracting the liquids and found phase separation at 900 °C. We hypothesize that the composition analysis of the alloys was performed in such a way that phase separation during quenching interfered with the results. Data below 800 °C agree with [52Cam] and other work.

We next considered the enthalpy of mixing data. Enthalpies of mixing [77Gir, 63Wit, 69Pre] as a function of

Table 2 Data on the Miscibility Gap

Reference	Compositions(a), at.% In L_1	L_2	Temperature, °C	Experimental method
[70Yaz](b)	···	85	685	emf
	···	75	760	
	···	55	848	
	···	40	(868)	
	25	···	(875)	
	10	···	812	
[66Mas](b)	···	88	660	emf
	···	85	735	
	···	80	810	
	···	70	842	
	···	60	842	
	···	50	(848)	
[52Cam]	5.5	83.4	675	Analysis of two liquids
	7.4	73.8	750	
	8.9	68.6	800	
	(14.1)	(48.9)	850	
[66Cam]	5.2	86.0	650	Analysis of two liquids
	7.9	86.4	700	
	10.5	77.3	750	
	10.4	72.1	800	
	(13.5)	(69.1)	850	
	(17.9)	(61.2)	900	
[69Zam]	···	80.2	725	Density
[65Pre]	5	···	637	DTA
	6.1	···	675	
	8.3	···	725	
	17.8	···	(812)	
	24.8	···	(825)	
	40	···	(830)	
	···	46.8	(828)	
	···	81.2	670	
	···	82.9	696	

(a) Data in parentheses are considered very uncertain. (b) These data sets, except data in parentheses, were used to determine phase boundaries.

composition lie on a straight line in the two-phase region. The break points on the Al-rich side of the miscibility gap are difficult to determine because the slope of the straight line is very close to that of the enthalpy in the single-phase region. Therefore, the enthalpy of mixing data was not used to derive phase boundaries.

The difficulty of interpreting emf data is that the slopes of the emf versus temperature for alloys of near critical compositions become equal. Moreover, at the critical point there is a change of slope of the emf versus temperature curve, which can be confused with the ordinary slope change at the phase boundary for alloys of noncritical composition. Electromotive force data are most unambiguous when several alloys on both sides of the critical composition are measured. From the data of [70Yaz], phase boundary data can be extracted unambiguously up to 850 °C, and the critical temperature can be estimated as between 870 and 880 °C. The critical composition can be estimated as 40 ± 5 at.% In. Similarly, for alloys between 85 and 60 at.% In, data can be unambiguously taken from [66Mas]. For a 50 at.% alloy, the temperature of the break point is uncertain. Again, the critical temperature is unambiguously placed above 850 °C.

Finally, we consider the DTA work of [65Pre], who placed the critical point at 830 °C. In a DTA measurement, a sharp break corresponding to a 15 J/mol·K discontinuity in the heat capacity is expected at the phase boundary (based on present calculations). The experimental difficulty is to ensure that the alloy is homogenized before beginning the run, either by stirring or by holding for a sufficient time above the miscibility gap. From [65Pre]'s observation that the heat effects were very small, we hypothesize that the alloys were heterogeneous at the beginning of the run and that the equilibrium miscibility gap was not observed.

Fig. 4 Extrapolation of the Miscibility Gap to the Critical Temperature

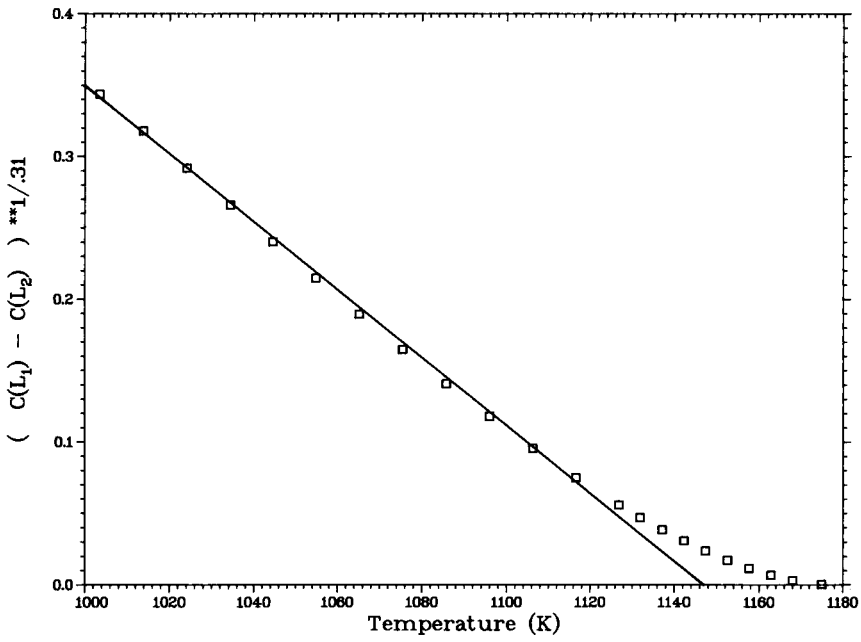

The points are values calculated by the classical model: near the critical point, the critical exponent becomes classical. The straight line extrapolation to the critical point was used to draw the assessed diagram (Fig. 1). J. L. Murray, 1983.

We, therefore, rely primarily on emf data for the miscibility gap together with the direct sampling data of [52Cam] for temperatures 800 °C and below. The phase boundary, Fig. 1, was arrived at by two steps: first, a thermodynamic analysis was performed, to be described below. The calculated critical temperature is 902 °C. This temperature must be higher than the true critical temperature because the classical Gibbs energy model gives an exponent of 0.5 rather than 0.31 for the phase boundaries in the critical region. Below T_c, an exponent of 0.31 is nearly approximated by the calculation over a wide temperature range. Next, a "calculated" critical point of 875 ± 5 °C was arrived at by extrapolating the noncritical region to $c_{L1} - c_{L2} = 0$. The procedure is illustrated in Fig. 4.

Solubility of In in (Al). The maximum solubility of In in (Al) is 0.045 at.% at the monotectic temperature, based on [55Sam].

Two metallographic studies were made of the (Al) solvus, using different specimen preparation techniques on the same alloy samples. [51Har] used the presence of etch pits as evidence of undissolved (In) particles. Segregation of In to the grain boundaries without precipitation may also cause similar etch pits, and it was therefore suggested that errors would tend to place the solubility lower than the equilibrium value. [55Sam] repeated the study, using a different polishing technique, and indeed found the solubilities to be slightly higher. Data of [55Sam] are given in Table 3. The assessed diagram is based on a ln c versus $1/T$ plot, which is expected to be linear for such dilute alloys. The plot deviates from a straight line only at the lowest temperature, 530 °C. Because failure to reach equilibrium or to observe very small precipitates may account for a too-high solubility at low temperatures, the higher temperature data are preferred, and the lower temperature solubility is adjusted from the original data accordingly.

In-Rich Alloys. Below 300 °C, the solubility of Al in the In-rich liquid is less than 0.2 at.% [47Val, 52Cam]. Reported temperatures of the reaction L → (In) + (Al) range between 155 and 156.3 °C [46Rau, 47Val, 48Kle, 48Dav, 49Pog, 52Cam]. The eutectic temperature in Fig. 1 is 156 °C.

Data on the (Al) liquidus between the monotectic and eutectic temperatures were reported by [66Mas], emf; [65Pre], DTA; [52Cam], quenching. There is no serious discrepancy among these determinations. The data are well represented by the present thermodynamic calculations, which have been used to draw the liquidus in Fig. 1.

Table 3 Solubility of In in (Al)

Temperature, °C	Experimental composition, at.% In	Assessed composition, at.% In
530	0.018	0.014
560	0.020	0.020
590	0.028	0.028
615	0.035	0.035
638	0.041	0.045

Data from [55Sam].

Metastable Phases

[55Sil] studied the aging of single crystals of (Al) containing 0.012 at.% In. Aging at temperatures below 300 °C resulted in a metastable fcc In-rich precipitate, denoted In′. It was not determined whether the precipitate was coherent with the matrix.

Systems with a liquid miscibility gap and monotectic reaction are favorable for the production of fibrous composite structures, and Al-In alloys were used in several solidification studies. Zero gravity solidification experiments verified that critical point wetting provides a mechanism for macrosegregation even in the absence of gravitational segregation [77Gel, 79Ahl]. [80Pot] compared microstructures formed during Bridgman, Czochralski, and isothermal solidification. [81Gru] showed that fibrous composite structures can be obtained by directional solidification at growth rates below 5 μm/s.

Crystal Structures and Lattice Parameters

Crystal structures and lattice parameters are summarized in Table 4. Lattice parameters of Al and In are from [Pearson], and of In′ from [55Sil]. Data on lattice parameters as a function of composition are not available because of the very low mutual solubilities.

Thermodynamics

Experimental Data. Enthalpies of mixing were measured by [77Gir], [63Wit], and [69Pre], and emf measurements of the Al partial Gibbs energies were made by [66Mas] and [69Yaz, 70Yaz, 71Lee].

The partial Gibbs energies have been used in this assessment primarily as phase boundary data (see "Equilibrium Diagram"). Partial Gibbs energies from the present calculations agree with the two emf determinations (within an error of, at most, about 400 J/mol).

Enthalpy of mixing data fall into two sets, [63Wit] and [77Gir], which are consistent with each other and with the phase diagram, and [69Pre], which are higher than the former by as much as 2000 J/mol. Data of [69Pre] are also scattered (±750 J/mol at intermediate compositions).

Table 4 Al-In Crystal Structure Data

Phase	Maximum composition range(a), at.% In	Pearson symbol	Strukturbericht designation	Space group	Prototype	Lattice parameters, nm a	c
(Al)	0-0.045	*cF4*	*A1*	*Fm3m*	Cu	0.40496	···
(In)	~100	*tI2*	*A6*	*I4/mmm*	In	0.45979	0.49467
Metastable phase							
(In′)(b)	*μ*	*cF4*	*A1*	*Fm3m*	Cu	0.465 ± 0.005	···

(a) From the phase diagram. (b) Data from [55Sil].

Fig. 5 Comparison of Calculated and Experimental Enthalpies of Mixing

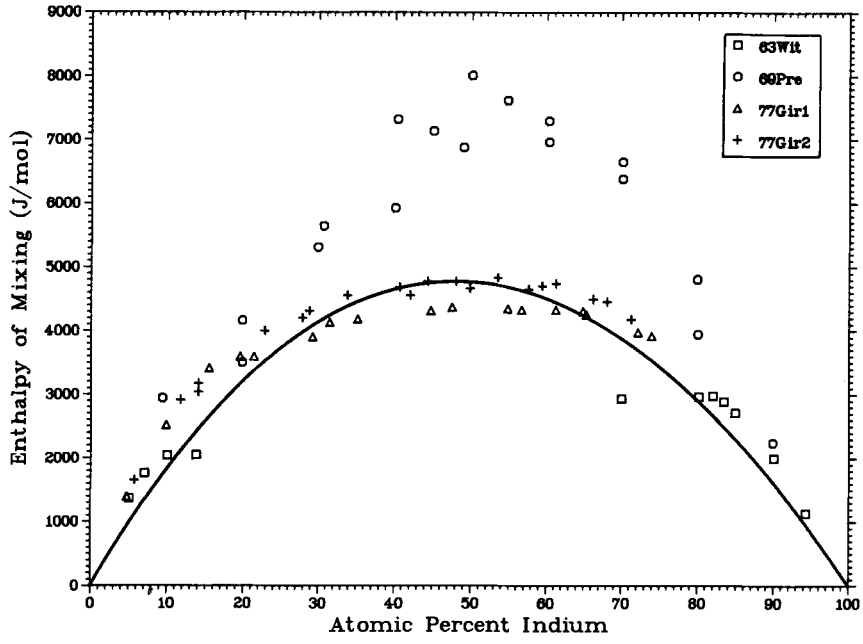

This calculation at 900 °C. J.L. Murray, 1983.

For the present optimizations, we used enthalpy of mixing data from [77Gir, 63Wit] for compositions in the single-phase field. All the enthalpy of mixing data, including points not used for the optimizations, are compared to the present calculations in Fig. 5.

Previous Phase Diagram Calculations (Liquid-Phase Gibbs Energy). Expressions for the liquid-phase excess Gibbs energy were reported by [72Gok, 74Per, 78Ans, 81Kau].

[72Gok] and [74Per] computed Gibbs energies based on phase boundary data only. [72Gok] used the phase diagram from [Hultgren] with a critical temperature of 852 °C. Calculated mixing enthalpies are low compared to experimental values because a relatively low critical point was chosen as a constraint. [74Per] derived Gibbs energies (using a Lumsden model) from phase diagram data of [52Cam] and [66Cam]. Calculated mixing enthalpies are large compared to experimental values because the critical temperature extrapolated from the phase boundary data is high: 975 °C.

On the other hand, [78Ans] optimized seven parameters of a polynomial expansion of the Gibbs energy with respect to enthalpy of mixing and partial Gibbs energy data [63Wit, 77Gir, 70Yaz, 66Mas]. The resulting Gibbs energy agrees with the enthalpy of mixing data within about 250 J/mol and with heats of mixing derived from [66Mas] within 900 J/mol. The Gibbs energy function is included in Table 5. This calculation provides a good representation of the enthalpies of mixing and predicts a critical temperature of about 850 °C. However, the calculation also has limitations that should be recognized when these parameters are used for further work: first, the low critical point is achieved at the expense of disagreement with phase diagram data for the Al-side of the phase diagram. This is reflected in a calculated monotectic point of (~6 at.% In, ~634 °C). Second, the excess entropy is determined by partial Gibbs energies almost exclusively at In-rich compositions. Because of the extrapolation to Al-rich compositions, this calculation appears to overemphasize partial Gibbs energy data.

[81Kau] based a polynomial Gibbs energy on the analysis of [78Ans], simplifying the seven-parameter representation to a four-parameter representation. The calculated monotectic point is (7 at.% In, 622 °C) and the critical point is 907 °C. [81Kau] also provided estimates of the melting entropy and enthalpy of metastable fcc In. These lattice stabilities are included in Table 5.

Table 5 Thermodynamic Properties of the Al-In System, J/mol, J/mol·K

Lattice stabilities of the pure components

$G^{Al}(L \rightarrow fcc) = -10\,795 + 11.565\,T$	From [Hultgren]
$G^{In}(L \rightarrow tet) = -\ 3\,264 + \ 7.594\,T$	From [Hultgren]
$G^{In}(L \rightarrow fcc) = -\ 2\,908 + \ 7.113\,T$	From [81Kau]

Liquid-phase Gibbs energy

[78Ans](a)

$H^{xs} = x(1 - x)[19\,188 + 2561\,\delta x + 7996\,\delta x^2]$
$S^{xs} = x(1 - x)[-1.2443 + 1.2481\,\delta x + 5.4392\,\delta x^2 - 0.8351\,\delta x^3]$

Present calculations(b)

$E_{Al}(i) = -587.3\,i + 313.6\,i^2$
$E_{In}(j) = -587.3\,j + 361.0\,j^2$

(a) x = atom fraction In, $\delta x = (1 - 2x)$. (b) See text for description of the Mathieu model.

Present calculations attempt to complement the previous thermodynamic analysis of this system. Three goals were set for the calculations:

- To give suitable weight to all the available data, emphasizing phase boundary data up to 800 °C and enthalpy of mixing data over the entire range. This goal was realized by making simultaneous optimizations with respect to these two data types.
- To account, although in a primitive and still classical way, for correlations associated with critical phenomena.
- To use the fewest possible parameters, in order to make use of the predictive nature of calculations for this controversial system.

The latter considerations were addressed by the use of the Mathieu model ("*atome entouré*"). In this model, we parametrize the potential energies of atoms surrounded by Z near-neighbors as a function of the number of unlike neighbors:

$$E_{Al} = A\,i + B_{Al}\,i^2 \qquad E_{In} = A\,j + B_{In}\,j^2$$

where i and j are numbers of unlike neighbors for Al and In, respectively. A and B are the energy parameters to be optimized. Z has been set to 10, based on the experimental work of [75Hoe]. The excess functions are calculated using a quasichemical-type approximation for the entropy. For B equals zero, this model reduces to the quasichemical model, and the excess quantities can be written in closed form; otherwise, they are calculated numerically. Details of the theory and examples for ordering systems are elaborated by [65Mat].

Comparisons of the calculated phase diagram and enthalpy of mixing with the experimental data are made in Fig. 3 and 5. The calculated critical point is (37.5 at.% In, 902 °C). The calculated monotectic point is (4.96 at.% In, 638 °C), and the composition of the second liquid at the monotectic temperature is 88.5 at.% In. The calculated excess entropies agree closely with excess entropies calculated using a polynomial model, with additional parameters explicitly describing the entropy terms. As discussed above, the calculated critical temperature should overshoot the true critical temperature, and corrections to the phase boundaries can be made by extrapolation into the critical region.

Cited References

46Rau: E. Raub and M. Engel, "Alloys of Al with Indium and Thallium", *Z. Metallkd.*, *37*, 148-149 (1946) in German. (Equi Diagram; Experimental)

47Val: S. Valentiner and I. Puzicha, "The System Aluminum-Indium", *Z. Metallkd.*, *38*, 127-128 (1947) in German. (Equi Diagram; Experimental)

48Kle: W. Klemm, L. Klemm, F. Hohmann, H. Volk, E. Orlamunder, and H.A. Klein, "The Behavior of Group III Elements Alloyed with Each Other and with Group IV Elements", *Z. Anorg. Chem.*, *256*, 240-241 (1948) in German. (Equi Diagram; Experimental)

49Pog: S.A. Pogodin, "The Aluminum-Indium Phase Diagram", *Izv. Sekt. Fiz.-Khim. Anal.*, *17*, 200-203 (1949) in Russian. (Equi Diagram; Experimental)

***51Har:** H.K. Hardy, "The Solid Solubilities of Cadmium, Indium, and Tin in Aluminum", *J. Inst. Met.*, *80*, 431-434 (1951). (Equi Diagram; Experimental)

***52Cam:** A.N. Campbell, L.B. Buchanan, J.M. Kuzmak, and R.H. Tuxworth, "The System Aluminum-Indium-Tin", *J. Amer. Chem. Soc.*, *74*, 1962-1966 (1952). (Equi Diagram; Experimental)

***55Sam:** L.E. Samuels, "The Solid Solubilities of Tin, Indium, and Cadmium in Aluminum", *J. Inst. Met.*, *84*, 333-336 (1955). (Equi Diagram; Experimental)

55Sil: J.M. Silcock, "Intermediate Precipitates in Aged Binary Alloys of Aluminum with Cadmium, Indium, or Tin", *J. Inst. Met.*, *84*, 19-22 (1955). (Meta Phases; Experimental)

***63Wit:** F.E. Wittig and G. Keil, "Heats of Mixing of Liquid Al Alloys with the B-Metals Zinc, Cadmium, Indium, Thallium, Tin, Lead, and Bismuth", *Z. Metallkd.*, *54*(10), 576-590 (1963) in German. (Thermo; Experimental)

65Pre: B. Predel, "Constitution and Thermodynamics of Miscibility Gap Systems", *Z. Metallkd.*, *56*(11), 791-798 (1965) in German. (Equi Diagram; Experimental)

***66Cam:** A.N. Campbell and R. Wagemann, "The System: Aluminum-Indium-Silver, Part I. The Binary and Ternary Miscibility Gaps", *Can. J. Chem.*, *44*, 657-660 (1966). (Equi Diagram; Experimental)

***66Mas:** G. Massart, F. Durand, and E. Bonnier, "Thermodynamic Study of Al-In Alloys Containing 1 to 60 at.% Aluminum", *C.R. Acad. Sci. Paris C*, *262*, 185-188 (1966) in French. (Thermo; Experimental)

69Pre: B. Predel and H. Sandig, "Thermodynamic Study of the Systems Aluminum-Bismuth, Aluminum-Indium, and Copper-Thallium", *Mater. Sci. Eng.*, *4*, 49-57 (1969) in German. (Thermo; Experimental)

***69Yaz:** A. Yazawa and Y.K. Lee, "Thermodynamic Study of Molten Aluminum-Indium Alloy", *J. Jpn. Inst. Met.*, *33*(3), 318-323 (1969) in Japanese. (Thermo; Experimental)

69Zam: S. Zamarca, I. Ganovici, and L. Ganovici, "Evidence of the Ternary Miscibility Gap in Indium-Aluminum-Silver System by Viscosity Measurements", *Rev. Rom. Chim*, *14*(2), 173-781 (1969). (Equi Diagram; Experimental)

70Yaz: A. Yazawa and Y.K. Lee, "Thermodynamic Studies of the Liquid Aluminum Alloy Systems", *Trans. Jpn. Inst. Met.*, *11*, 411-418 (1970). (Thermo; Experimental)

***71Lee:** Y.K. Lee, "Thermodynamic Properties of Liquid Aluminum-Indium System", *J. Korean Inst. Met.*, *8*(4), 205-211 (1971) in Korean. (Thermo; Experimental)

72Gok: N.A. Gokcen and E.T. Chang, "Liquid-Liquid Equilibria and Gibbs Energy of Mixing for Binary Systems", *Scr. Metall.*, *6*, 249-252 (1972). (Thermo; Theory)

74Per: A.E.C. Peres and V.F. Campos, "Thermodynamic Study of the Pb-Zn and Al-In Systems", *Metal. ABM*, *194*(3), 13-18 (1974) in Portuguese. (Thermo; Theory)

75Hoe: J. Hoehler and S. Steeb, "Structure of Al-In Melts by X-Ray Wide Angle Scattering", *Z. Naturforsch.*, *30*(A), 771-774 (1975) in German. (Thermo; Experimental)

77Gel: S.H. Gelles and A.M. Markworth, "Agglomeration in Immiscible Liquids", Appl. of Space Flight in Matls. Sci. and Technol., NBS Spec. Publ. 520, S. Silverman and E. Passaglia, Ed., 51-58 (1977). (Meta Phases; Experimental)

77Gir: C. Girard, R. Baret, J.P. Bros, and P. Leydet, "Enthalpy of Formation of the Ternary Liquid Alloy Al-Ga-In", *J. Chim. Phys.*, *74*(10), 1061-1068 (1977) in German. (Thermo; Review)

78Ans: I. Ansara, J.P. Bros, and C. Girard, "Thermodynamic Analysis of the Ga-In, Al-In and Al-Ga-In Systems", *Calphad*, *2*(3), 187-196 (1978). (Thermo; Theory)

79Ahl: H. Ahlborn and K. Lohberg, "Aluminum-Indium-Experiment SOLUOG-A Sounding Rocket Experiment on Immiscible Alloys", Amer. Inst. of Aero. and Astro.; Aerospace Science Meeting, 17th, New Orleans, LA (1979). (Meta Phases; Experimental)

80Pot: C. Potard, "Solidification Structures in Immiscible Alloys Al-In and Al-Cd", *Ann. Chim. Fr.*, *5*, 279-287 (1980) in French. (Meta Phases; Experimental)

81Gru: R.N. Grugel and A. Hellawell, "Alloy Solidification in Systems Containing a Liquid Miscibility Gap", *Metall. Trans. 12A*, 669-681 (1981). (Meta Phases; Experimental)

81Kau: L. Kaufman, J. Nell, K. Taylor, and F. Hayes, "Calculation of Ternary Systems Containing III-V and II-VI Compound Phases", *Calphad*, *5*(3), 185-215 (1981). (Thermo; Theory)

*Indicates key paper.

Al-In evaluation contributed by **Joanne L. Murray,** Center for Materials Science, National Bureau of Standards. This work was jointly funded by the Defense Advanced Research Project Agency (DARPA) and the National Bureau of Standards through the Metallurgy Division and through the Office of Standard Reference Data. The author would like to thank John Cahn for many fruitful conversations about critical phenomena in this system, and Daniel Kahan for his contributions to the data compilation effort. Literature searched through 1980. Dr. Murray and Dr. A.J. McAlister are the ASM/NBS Data Program Category Editors for binary aluminum alloys.

The Au-Ti (Gold-Titanium) System

196.9665 47.88

By J. L. Murray
National Bureau of Standards

Equilibrium Diagram

The main outlines of the Ti-Au system are the result of two studies [56Pie, 62Pie]. Additional data from [78Pli, 63Hah, 70Don, 62Sto, 54Mcq] corroborate and refine the findings of [56Pie, 62 Pie]. Thermodynamic calculations of the diagram agree very well with direct phase boundary data, within errors expected for a Ti-based system for which there are no experimental thermodynamic data. The calculated and assessed diagrams agree within ±35 °C for the invariant temperatures of the three-phase equilibria, and they are usually much closer. In the assessed diagram shown in Fig. 1, the (Au) boundaries were drawn using the thermodynamic calculation because they agreed with the assessment within 2 °C; the (βTi) liquidus and solidus were based on calculations because the experimental results do not conform with thermodynamic constraints. The rest of the assessed diagram was fitted directly to the experimental data.

The equilibrium solid phases of the Ti-Au system are:

- The bcc (βTi) solid solution, with a maximum Au solubility of about 15 at.%.
- The cph (αTi) solid solution, with a maximum Au solubility of about 1.7 at.%.
- The fcc (Au) solid solution, with a maximum Ti solubility of 12 at.%.
- The stoichiometric compound Ti_3Au, with the *A*15 structure and a congruent melting point.
- The equiatomic TiAu compounds, with a maximum solubility range of 38 to 52 at.% Au. The allotropic forms with the CsCl, AuCd, and γTiCu structures are designated γTiAu, βTiAu, and αTiAu, respectively.
- The stoichiometric compound $TiAu_2$, with the $MoSi_2$ structure and a congruent melting point.
- The compound $TiAu_4$, with composition range 79 to 82 at.% Au. $TiAu_4$ has the Ni_4Mo structure and melts by a peritectic reaction with (Au).

Fig. 1 Assessed Ti-Au Phase Diagram

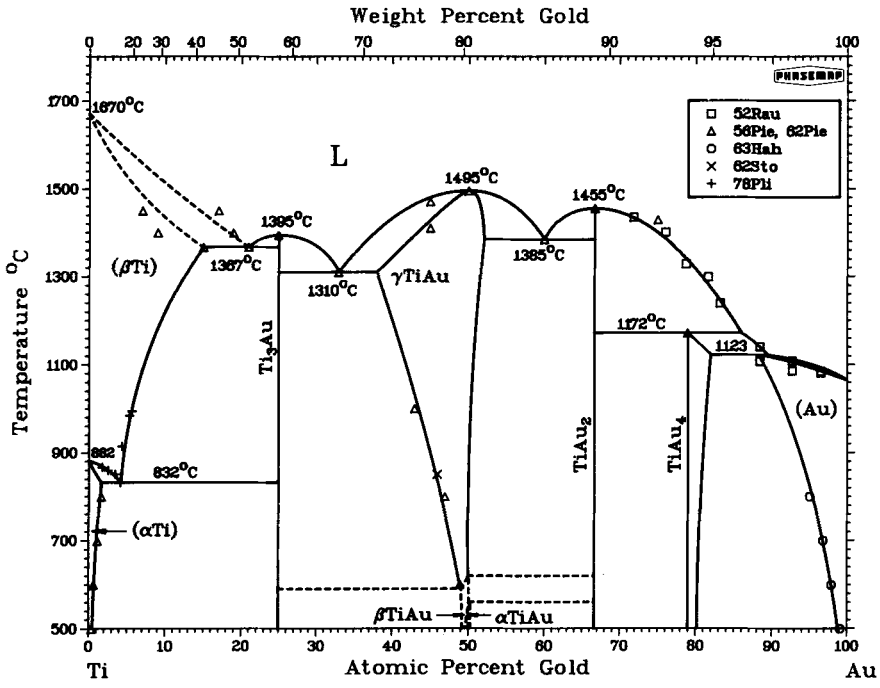

Compared to selected experimental data.

J. L. Murray, 1983.